



Deeper insights into the effects of substrate to inoculum ratio selection on the relationship of kinetic parameters, microbial communities, and key metabolic pathways during the anaerobic digestion of food waste

Yanzeng Li^{a,b}, Zhou Chen^{a,b}, Yanyan Peng^a, Weizhao Huang^c, Junxiao Liu^c, Vladimir Mironov^d, Shenghua Zhang^{a,*}

^a Key Lab of Urban Environment and Health, Institute of Urban Environment, Chinese Academy of Sciences, Xiamen 361021, China

^b University of Chinese Academy of Science, Beijing 100049, China

^c Lianyijiyuan Environmental Protection Engineering Co. Ltd, Xiamen 361021, China

^d Winogradsky Institute of Microbiology, Research Center of Biotechnology, Russian Academy of Sciences, Moscow, Russia

ARTICLE INFO

Keywords:

Food waste
Anaerobic digestion
Substrate to inoculum ratio
Microbial communities
Metabolic pathways

ABSTRACT

The substrate to inoculum ratio (S/I) is a crucial factor that affects not only the stability of the anaerobic digestion (AD) of food waste (FW) but also the methanogenic capacity of the substrate. This is of great significance for the start-up of small-scale batch reactors and the directional regulation of methanogenesis and organic acid production. Most studies have merely clarified the optimal S/I ratio for methane production and revealed the basic composition of microbial communities. However, the mechanism of microbial interactions and the metabolic pathways behind the optimal S/I ratio still remain unclear. Herein, the effects of different S/I ratios (VS basis) on the relationship of kinetic parameters, microbial communities, and metabolic pathways during the AD process of FW were holistically explored. The results revealed that high S/I ratios (4:1, 3:1, 2:1, and 1:1) were prone to irreversible acidification, while low S/I ratios (1:2, 1:3, and 1:4) were favorable for methanogenesis. Moreover, a kinetic analysis demonstrated that the methane yield of S/I = 1:3 were the highest. A bioinformatics analysis found that the diversity of bacteria and archaea of S/I = 1:3 were the most abundant, and the enrichment of *Bacteroides* and *Synergistetes* could help to establish a syntrophic relationship with hydrogenotrophic methanogens, which could aid in the fulfillment of a unique niche in the system. In contrast to the findings with the other S/I ratios, the cooperation among microbes in S/I = 1:3 was more apparent. Notably, the abundances of genes encoding key enzymes involved in the methanogenesis pathway under S/I = 1:3 were all the highest. This knowledge will be helpful for revealing the influence mechanism of the ratio relationship between microorganisms and substrates on the biochemical metabolic process of anaerobic digestion, thereby providing effective guidance for the directional regulation of FW batch anaerobic reactors.

1. Introduction

Anaerobic digestion (AD) has been widely proven to be an economically efficient means for the disposal of organic waste, such as food waste, sludge, and animal waste, among others. Organic macromolecules are catabolized by anaerobic microorganisms to generate CH₄ and CO₂, accompanied by a large number of value-added chemicals, such as volatile fatty acids (VFAs), lactic acid (LA), and ethanol (Lin et al., 2018). A large amount of biogas slurry (BS) is typically produced during the process of AD of organic waste. Lu and Xu. (2021) found that

approximately 0.20 to 0.47 tons of digestate is produced during the AD of FW per ton, in which BS is the main part. BS contains a variety of microorganisms and N and P elements, and its pH value is typically stable between 7.0 and 8.0. Thus, this BS can be used as a suitable inoculum for the start-up of anaerobic reactors. Kong et al. (2016) found that when FW BS served as the inoculum, the cumulative yield of CH₄ could reach as high as 580 mL/g VS_{added}, which was higher than when sewage sludge was used as the inoculum. Zhou et al. (2016) found that the maximum production of CH₄ can reach 16,607 mL at pH 7.0 using BS from pig manure as inoculum.

* Corresponding author.

E-mail address: shzhang@iue.ac.cn (S. Zhang).

<https://doi.org/10.1016/j.watres.2022.118440>

Received 22 October 2021; Received in revised form 6 April 2022; Accepted 7 April 2022

Available online 9 April 2022

0043-1354/© 2022 Elsevier Ltd. All rights reserved.

As described above, the BS produced by the AD of organic waste can be used as the inoculum for the start-up of FW anaerobic reactors, which can not only provide the key microorganisms for hydrolysis, acidogenesis and methanogenesis, but also recycle the waste. S/I is an important parameter affecting the stability of batch AD. An S/I ratio that is too high could cause toxicity, destroy the syntrophy between microbes, and irreversibly acidify the reactor. A lower S/I ratio can prohibit the induction of enzymes required for AD, and the maximum methane production cannot be achieved (Kong et al., 2016; Xing et al., 2020). The identification of an optimal S/I ratio in AD has been widely studied and has primarily focused on two subsequent perspectives. The first was to determine the most suitable S/I ratio for methanogenic efficiency by establishing a kinetic model. Xing et al. (2020) reported that $S/I < 0.07$ is the most suitable ratio for the early start-up operation of anaerobic reactors for the co-digestion of FW and cow manure. Li et al. (2018b) found that the cumulative yield of methane can reach a maximum of 1075 mL/g VS at $S/I = 0.6$ during the co-digestion of FW and sludge. The second was to elucidate the community structure under the optimal S/I ratio using 16S rRNA sequencing technology. Meng et al. (2018) investigated the community composition of the optimal S/I ratio for CH₄ production ($S/I = 0.5$, 661 m³/t VS) in the co-digestion of pig urine and rice straw and found that the corresponding dominant microorganisms were *Clostridia*, *Methanosarcina*, and *Methanothermobacter*. Ma et al. (2019a) reported that $S/I = 2:3$ was the most effective methanogenic ratio (209.1 mL/g VS_{added}) in a study of the co-digestion of dairy manure and rapeseed straw, and the predominant microorganisms in the community were *Proteobacteria*, *Bacteroidetes*, and *Methanosaeta*. It is thus apparent that the optimal S/I ratio differs in different studies. The nutrient composition of substrate and the physicochemical properties and microbial characteristics of inocula vary widely, which could directly affect the results of studies to explore the S/I ratio. Moreover, different S/I ratios can affect the key microorganisms and intermediate metabolites in AD, resulting in variation in the functional metabolic pathways. However, the mechanism of microbial interactions and functional metabolism under the optimal S/I ratio during the process of AD of FW still remain unclear.

Key microorganisms can drive changes during the process parameters, thus, affecting the community composition and functional metabolism in AD (Wang et al., 2018). A bioinformatics analysis can be applied to identify key microorganisms in complex communities and deduce the correlation between microbes. For instance, random forest analysis has been verified to be one of the exact tools in machine language to describe the systematic importance of each taxon (Long et al., 2021). This type of analysis can be utilized to analyze and predict the key microorganisms in the anaerobic system based on the R language software and quantify the importance of each taxon to the anaerobic system. Therefore, this analysis could reveal the relationship between key microorganisms and the performance of AD. The relationship between microbes in the network can be constructed using a microbial correlation network analysis, which can intuitively illustrate the interactions between microorganisms and thereby identify the key microorganisms that drive the changes in community composition and function (Zheng et al., 2021).

The prediction of metabolic pathways can predict the in-depth metabolic functions owing to the perspective of expression of key functional genes. Tax4Fun software can predict the spectrum of gene functions of the whole spectral system of bacteria and archaea based on the Kyoto Encyclopedia of Genes and Genomes (KEGG) metabolic pathway database, which helps to predict the functional metabolic pathways and the key enzymes of each group. The Tax4Fun function prediction has been widely used in the studies of AD processes. Zheng et al. (2021) compared the metabolic pathways of the co-digestion of pig manure and corn stover under different C/N based on Tax4Fun software. Ma et al. (2021) also investigated the changes in the methanogenic functional genes during a study on the effects of magnetite on saline wastewater AD. However, although Tax4Fun software can be used to

clarify the entire metabolic pathways in AD, it still lacks the corresponding annotation on the key microbes in metabolic pathways. Using both random forest and microbial correlation networks can effectively remedy this defect, thus helping to elucidate the differences in metabolic function and community structure at each S/I ratio.

Therefore, the objective of this study was to clarify the AD performance of FW at different S/I ratios, and then comprehensively analyze the microbial interactions and whole metabolic pathways under the optimal S/I ratio. Firstly, the kinetic parameters of hydrolysis and methanogenesis under each S/I ratio were analyzed, and acidogenesis at the corresponding ratios was discussed. Afterwards, the bacterial and archaeal community structure were analyzed using random forest and correlation network analyses. Finally, comprehensive insights were used to reveal the functional metabolic pathways of hydrolysis, acidogenesis, and methanogenesis under the optimal S/I ratio. The mutual corroboration of these results facilitates the selection of the optimal S/I ratio, thereby maximizing the synergistic actions between the substrate and the inoculated microorganisms.

2. Materials and methods

2.1. Substrate and inoculum

To ensure the homogeneity of the substrate, the FW used in this research was synthesized by selecting widely representative food ingredients based on the component analysis of our previous study (Chen et al., 2021). The main ingredients were rice (35%), lean meat (10%), fat (20%), fish (3.3%), chicken (8.3%), soybeans (6.7%), celery (8.3%), and cabbage (8.3%). These ingredients were crushed to 1~2 mm using a food grinder and stored at -20 °C. The BS was collected from the FW anaerobic tank (Xiang'an East Solid Waste Treatment Plant, Xiamen, China). The hydraulic retention time of the AD tank was 30 days, and the daily intake of FW was approximately 440 m³, which is similar to the amount of BS that was discharged daily. After the BS was discharged from the tank, it entered the sewage treatment process of the plant. Table 1 shows the composition and characteristics of FW and BS.

2.2. Experiment design

The S/I ratio based on the volatile solid was established at 4:1, 3:1, 2:1, 1:1, 1:2, 1:3, and 1:4, respectively. The FW and BS were mixed at 500 g. The carbon to nitrogen ratio (C/N) of the mixture was maintained at approximately 15. The blank, without any substrate, was only inoculated with inoculum. All experiments were performed in triplicate. The methane production at each S/I ratio was calculated by subtracting the methane production of the blank, which was normalized to the Standard Temperature and Pressure (STP) conditions (273.15 K and 1 atm) (Holliger et al., 2016; Khadka et al., 2022). Each anaerobic bottle was connected to a 2 L gas sampling bag through a latex tube. Nitrogen was introduced into each bottle for 5 min before the experiment, and the air in the bottle was removed to ensure that its state was absolutely anaerobic. After that, the bottles were placed in a thermostat water bath vibrator (SHA-BA; China) with a speed of 120 rpm, and the temperature was established at 37 ± 1 °C. The pH was controlled at 7.0 ± 0.2 in the initial stage, and the pH of the material was adjusted with 5.0 M NaOH and 2.0 M HCl. The gas content was measured daily. The digestion was deemed to be terminated when there was no significant difference in the production of methane. A portion of the collected samples were stored at 4 °C to determine the physical and chemical properties, and the other portion was frozen at -80 °C for the microbial community analysis.

2.3. Analytical methods

2.3.1. Physical and chemical analysis

A CNS element analyzer (Vario MAX, Germany) was used to analyze the total carbon (TC), total nitrogen (TN), and carbon-nitrogen ratio (C/

Table 1
The composition and characteristics of FW and BS.

	FW	BS
pH	6.75±0.00	8.02±0.00
VS(%)	99.00±2.59	66.67±13.33
C(%)	56.54±0.56	27.84±1.14
N(%)	4.06±0.03	4.56±0.25
C/N	13.94±0.12	6.09±0.11
VFAs (g/L)	0.83±0.03	0.18±0.08
Lactic acid (g/L)	8.51±2.52	0.18±0.08
NH ₄ ⁺ -N (g/L)	0.25±0.00	3.19±0.02
SCOD (g/L)	16.80±2.30	7.10±1.05
Lipid (mg/g)	400.84±11.53	Not determined
Protein (mg/g)	55.66±7.37	Not determined
Starch (mg/g)	322.63±27.14	Not determined

N). The measurements of oil and fat were determined using a Sors extractor (NAI-ZFCDY-4Z; China). The contents of starch and soluble proteins were determined using a starch kit and Coomassie bright blue protein kit (YX-W-C400 and YX-W-C202; Sinobestbio, Shanghai, China). The contents of SCOD and NH₄⁺-N were determined by an analysis of water quality (APHA, 2005). The samples were dried to a constant weight in a 105 °C oven to measure the total solid (TS). The oven-dried samples were further heated for 3 h at 550 °C to determine the volatile solid (VS). The pH was determined by a Hashdo parameter portable water quality analyzer (HQ40D; USA). The detailed analytical methods for CH₄, VFAs, and LA are explained in the Supplementary Information. All the samples were analyzed in triplicate.

2.3.2. Microbial community analysis

Samples were collected at the end of the batch experiment for DNA extraction. A microbiological analysis was used to explore the structure of microbial communities and reveal the key metabolic pathways under the optimal S/I ratio. This analysis was performed on the group with the highest acid production S/I = 4:1 and the three groups with relatively high methane production S/I = 1:2, 1:3, and 1:4. Each group was designated as T1, T2, T3, and T4, respectively. Microbial DNA was extracted using HiPure Soil DNA Kits (Magen, Guangzhou, China). After the DNA had been extracted, the V3-V4 region of the bacterial 16S rRNA genes was amplified using the primers 341F (5'-CCTACGGGNGGCWGCAG-3') and 806R (5'-GACTACHVGGGTWTCTA AT-3'). The Arch519F (5'-CAGCMGCCGCGGTAA-3') and Arch915R (5'-GTGCTCCCCGC CAATTCCT-3') primers were used to amplify the archaeal 16S rRNA V4-V5 region. The purified amplification products were analyzed on an Illumina platform (Novaseq 6000; Gene Denovo, Guangzhou, China). The bioinformatics analysis is shown in the Supplementary Information.

2.3.3. Kinetic analysis

The kinetic models employed in this research were first order kinetic model and modified Gompertz model, and the detailed operations are shown in the Supplementary Information.

2.4. Statistical analysis

All experiments were performed in triplicate, and the results were expressed as mean ± standard deviation (standard deviation of technical replicates). Data processing was conducted using Microsoft Excel 2019. Statistical significance was determined by analysis of variance (ANOVA) using SPSS 22.0. AD performance and microbial communities of different S/I were compared using one-way ANOVA, and multiple comparison between groups were performed using Least Significant

Difference (LSD) method. All the results were considered to be statistically significant at $P < 0.05$. Origin 2021 and Adobe Illustrator CS5 were used to draw the graphics. A kinetic analysis was performed in Origin 2021. A random forest algorithm analysis was conducted in R programming language 3.4.1. A correlation network was performed using Gephi 0.9.2 software. The microbial analysis platform used was Omicsmart Platform (<https://www.omicsmart.com/>).

3. Results and discussion

3.1. Influence of different S/I ratios on AD performance

To explore the influence of different S/I ratios on the performance of AD, the kinetics of hydrolysis and methanogenesis were analyzed, and changes in the composition of VFAs, production of LA, and pH were discussed.

3.1.1. Kinetic models analysis

The VS content of the low S/I ratios (1:2, 1:3, and 1:4) decreased by approximately 30%; this reduction was greater than those of the high S/I ratios (4:1, 3:1, 2:1, and 1:1) ($P < 0.05$) (Fig. 1a). This finding indicated that an appropriate increase in the proportion of inoculum helps to degrade FW. A first-order kinetic model was utilized to characterize the hydrolytic process under different S/I ratios ($R^2 \geq 0.82$) (Table 2). The K_d of S/I = 4:1 ($0.21 d^{-1}$) was higher than those of S/I = 3:1 ($0.16 d^{-1}$) and 2:1 ($0.19 d^{-1}$). Li et al. (2018a) found that when the biomass concentration was 5 g VSS/L, the K_d of substrate concentration was 20 g VS/L, which was greater than at 10 and 15 g VS/L. Moreover, S/I = 4:1 contained more organic components, which provided a substantial carbon source for lactic acid bacteria, resulting in the continuous production of LA and a gradual decrease in pH (Fig. 2b-2c). Wu et al., 2016 found that when the pH was between 4 and 5, the FW will be degraded by lactic acid bacteria to generate a large amount of LA, thereby clearly increasing the hydrolysis rate. It was clearly apparent that the K_d of S/I = 1:2, 1:3, and 1:4 (0.33, 0.25, and $0.29 d^{-1}$, respectively) was higher than those of the high S/I ratios ($P < 0.05$), and the K_d of S/I = 1:2 was the largest. Relevant studies have shown that pH values between 6.5 and 7.5 were more suitable for the growth of *Defluviitoga*, which acts as the predominant hydrolytic bacterium (Hania et al., 2012). In this case, the pH was weakly acidic (6.6–7.4) at S/I = 1:2 (Fig. 2f), and *Defluviitoga* was the most abundant (Fig. 3e).

During the whole AD process, the cumulative methane production of S/I = 1:2, 1:3, and 1:4 was 601.83, 1747.52, and 1624.73 mL, respectively, which was clearly higher than those of the high S/I ratios ($P < 0.05$) (Fig. 1b). This was primarily because the BS inoculum contained a large number of methanogens, which could facilitate the conversion of H₂, CO₂, and acetic acid to CH₄ (Kong et al., 2016; Wang et al., 2018). In addition, LSD between-group comparison showed that the cumulative production of CH₄ in S/I = 1:3 was significantly higher than that in the other two groups ($P < 0.05$). The growth and metabolism of the methanogens were the most vigorous at this ratio (Section 3.3). However, the production of methane was extremely low in the high S/I ratios. This discrepancy was owing to the longer process of hydrolysis and irreversible acidification at the high S/I ratios, which renders a change in hydrolysis and acidogenesis to become the limiting step in the process of methanogenesis, making it difficult to increase the cumulative production (Ma et al., 2019b).

Fig. 1c shows the variation in the daily yield of CH₄ at different S/I ratios. The daily yield of CH₄ at the high S/I ratios (4:1, 3:1, 2:1, and 1:1) all decreased. When the rates of hydrolysis and acidogenesis in the system were greater than that of methanogenesis, large numbers of VFAs were found to accumulate (Fig. 2c-2f), leading to a decrease in the daily rate of methane production (Wang et al., 2018). However, the daily yield of methane at S/I = 1:2, 1:3, and 1:4 increased first and then decreased during the digestion process. The methane yield of S/I = 1:2 reached its maximum on day 1, which was 27.21 mL/g VS, while the S/I

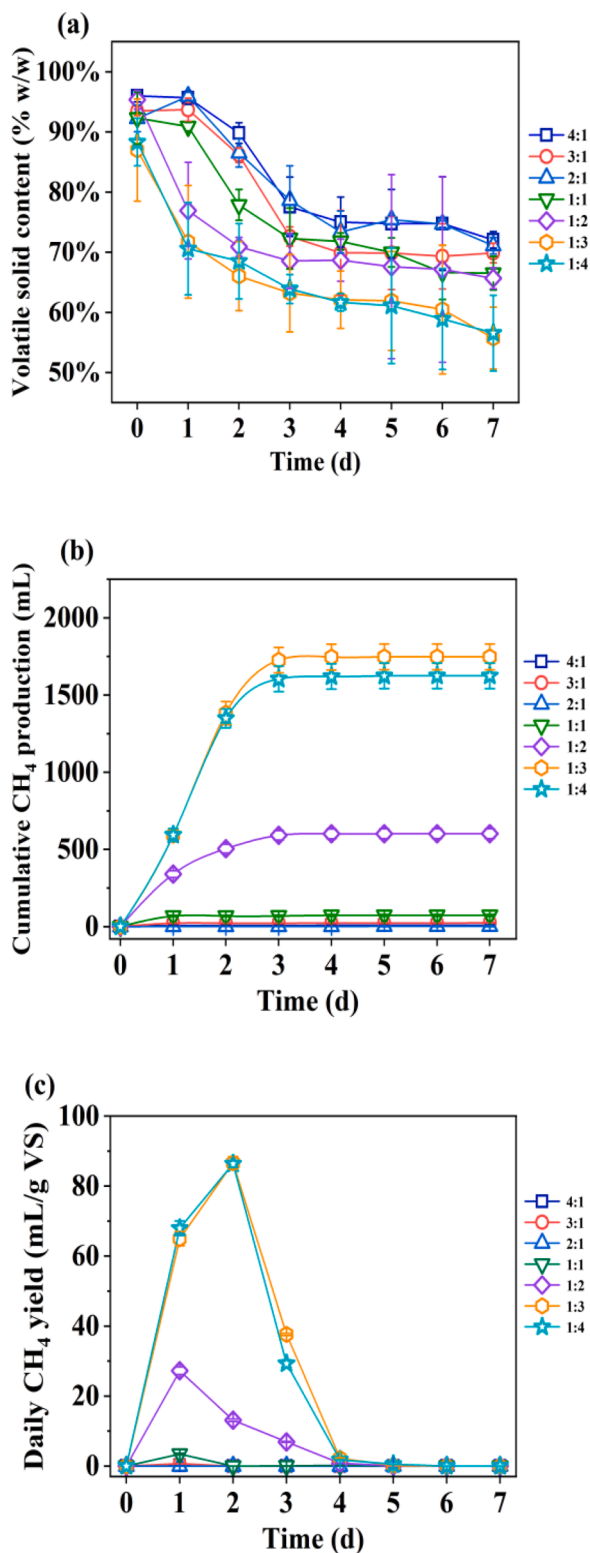


Fig. 1. The variation in (a) volatile solid, (b) cumulative production of methane, and (c) the daily yield of methane at different S/I ratios.

= 1:3 and 1:4 reached a peak by day 2, which was 86.63 and 86.36 mL/g VS, respectively. This was owing to the quick degradation of organic matter, which did not cause acidification, and provided a sufficient nutrient substrate and an appropriate environment for the methanogens to metabolize methane. As the digestion progressed, the available substrate was gradually reduced. Thus, the yield of methane gradually

declined. The discrepancy in the daily yield of methane during different S/I ratios was caused by the difference in the biodegradability of organic matter in FW and the BS that was inoculated (Ma et al., 2019b).

A modified Gompertz model was applied to fit the dynamic process of methanogenesis ($R^2 > 0.98$) (Table 2). The P_m and R_m of S/I = 1:2, 1:3, and 1:4 were significantly higher than those of the high S/I ratios ($P < 0.05$). Zhang et al. (2017) showed that lower K_d and R_m values indicated that the system was inhibited by the accumulation of acid (Fig. 2a-2b). The lag phase (λ) reflected the delayed response and subsequent adaptation of microorganisms to the constantly changing environment (Li et al., 2018a). The λ of S/I = 1:2 was the shortest (0.11 d), while the K_d ($0.33 d^{-1}$) at this ratio was the largest. This indicated that the hydrolytic bacteria can quickly respond to the changing environment, which enables the rapid start of methanogenesis (Mao et al., 2017). In addition, the λ of S/I = 1:3 and 1:4 was slightly higher than those of the high S/I ratios. Notably, in contrast to previous studies with a lag phase of 0.5 to 20.0 d (Cho et al., 2013; Kong et al., 2016; Zhang et al., 2017), the λ of each S/I ratio in this study was relatively short, which could be owing to the quicker production of methane and shorter digestion period (Xing et al., 2020; Zhang et al., 2017). The effective fermentation time (T_{ef}) is equal to the time taken for methane production to reach 90% (T_{90}) minus the λ . The T_{ef} of S/I = 1:3 and 1:4 was longer than that of the other groups (Table 2). A longer T_{ef} and shorter λ revealed that the conversion of organic matter was more efficiently converted into methane, and the production of methane was higher (Mao et al., 2017).

3.1.2. Changes in the concentrations of VFAs and LA and the pH under different S/I ratios

Fig. 2 illustrates the variation of VFAs, LA, and pH under different S/I ratios. The VFA concentrations at S/I = 1:2, 1:3, and 1:4 were higher than those of the other ratios before day 3 (Fig. 2a), which was consistent with the higher K_d . The concentrations of VFAs at the high S/I ratios (4:1, 3:1, 2:1, and 1:1) significantly increased since day 3 ($P < 0.05$). A large amount of LA could be converted into propionic acid by propionate dehydrogenase as the digestion of AD proceeded (Lee et al., 2008). The concentration of propionic acid clearly increased at high S/I ratios, while that of LA decreased dramatically (Fig. 2c-2f). Compared with high S/I ratios in the whole AD, the acid concentrations at S/I = 1:2, 1:3, and 1:4 were significantly lower. Thus, the corresponding pH was more stable (6.68–7.62). Li et al. (2018a) demonstrated that pH values between 6.5 and 8.2 are suitable for the growth and metabolism of methanogens.

The LA concentrations at S/I = 4:1, 3:1, 2:1, and 1:1 were significantly higher than those at low S/I ratios during the early stage ($P < 0.05$) (Fig. 2b), indicating that the synthesis of LA was the dominant acidogenesis pathway at high S/I ratios. In contrast, the accumulation of LA results in a dramatic decrease in the pH (4.55–5.37), which leads to irreversible acidification and difficulty in smoothly transforming to methanogenesis. An appropriate increase in pH aided the ability of lactic acid bacteria to synthesize LA. Tang et al. (2017) found that an appropriate increase from 4 to 5 in the pH aids in the stimulation in the production of LA. Therefore, from day 1 to day 2, the content of LA increased as the pH increased.

The acetic acid concentrations at S/I = 1:3 and 1:4 were maximal on day 1 (8.95 and 9.70 g COD/L, respectively), which were clearly higher than that of the other groups (Fig. 2c-2f), indicating that anabolism of acetic acid was the primary metabolic pathway of acidogenesis in S/I = 1:3 and 1:4 at this time. Moreover, the cumulative production of methane tended to increase significantly ($P < 0.05$) (Fig. 2b). Furthermore, although the concentrations of the acetic acid of S/I = 4:1, 3:1, 2:1, and 1:1 could reach 7.50–10.16 g COD/L, the cumulative methane production was significantly lower than that under the low S/I ratios. This could be because the sudden decrease in pH severely inhibited the process of the use of acetic acid by aceticlastic methanogens to produce methane. In addition to S/I = 1:3 and 1:4, the concentration of propionic

Table 2
Kinetic parameters under different S/I ratios.

S/I	First order kinetic		Modified Gompertz model				T_{90} (d)	T_{er} (d)	CH ₄ yield(mL/g VS)
	$K_d(d^{-1})$	R^2	P_m (mL)	R_m (mL/d)	λ (d)	R^2			
4:1	0.21	0.93	7.81	6.15	0.17	0.990	1.53	1.36	0.23
3:1	0.16	0.96	22.21	21.60	0.19	0.998	0.55	0.36	0.68
2:1	0.19	0.94	1.38	1.29	0.17	0.982	4.03	3.86	0.07
1:1	0.21	0.92	72.38	67.79	0.18	0.995	0.73	0.55	3.67
1:2	0.33	0.82	599.14	369.67	0.11	0.993	3.32	3.21	48.07
1:3	0.25	0.91	1759.23	1028.34	0.43	0.999	4.94	4.51	191.61
1:4	0.29	0.85	1630.66	1031.21	0.43	1.000	4.75	4.32	185.90

Note: ; P_m is the maximum cumulative production of methane (mL); R_m is the maximum rate of methane production (mL/d); t is the fermentation time (d); λ is the lag phase (d).

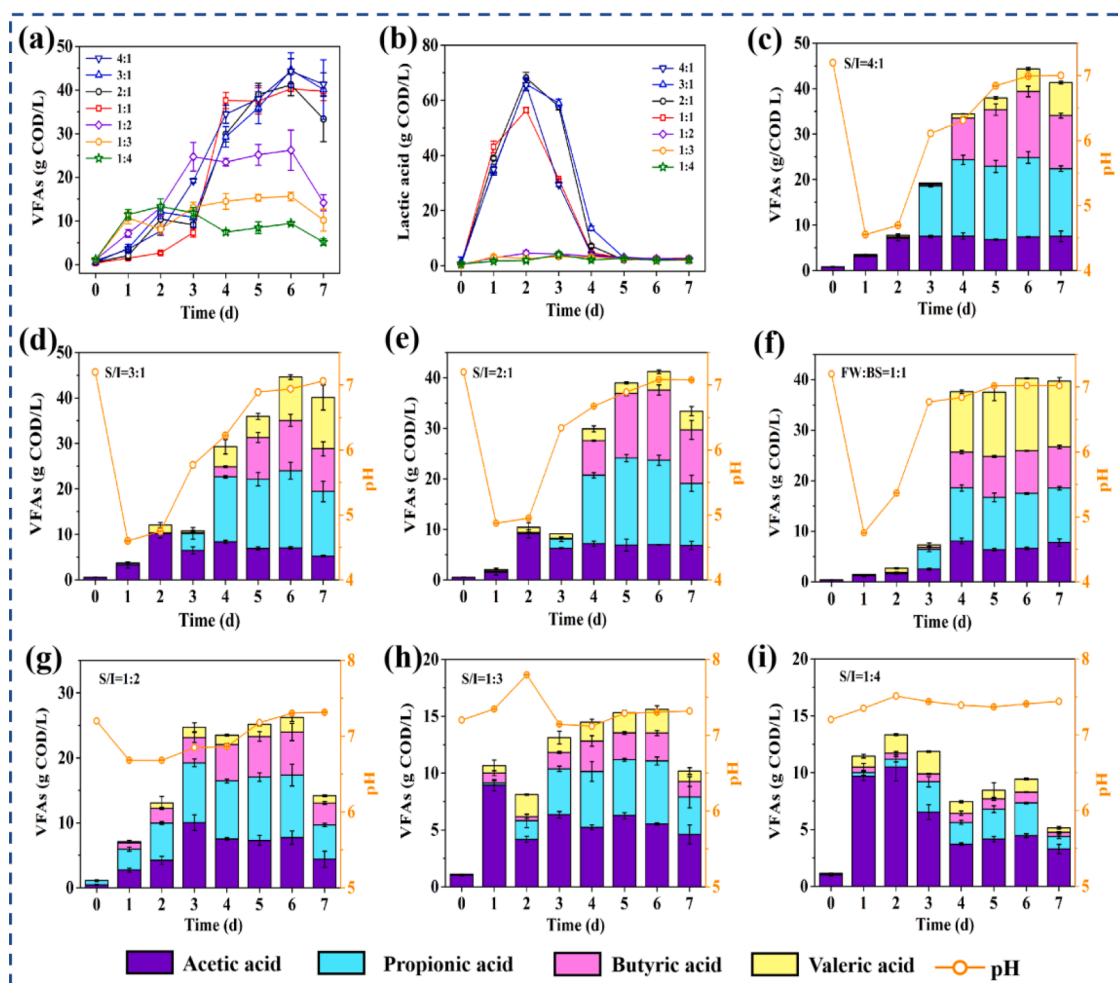


Fig. 2. The changes in (a) total VFAs (including acetic acid, propionic acid, butyric acid, and valeric acid), (b) LA (lactic acid), and (c-i) composition of VFAs and the pH under different S/I ratios: (c) 4:1, (d) 3:1, (e) 2:1, (f) 1:1, (g) 1:2, (h) 1:3, (i) 1:4.

acid in other groups was extremely high. Li et al. (2020) concluded that when the concentration of propionic acid exceeded 5 g COD/L, it strongly inhibited methanogenesis.

3.2. Microbial community structure analysis

In this study, a detailed community structure analysis was conducted on the $S/I = 4:1$ (T1) with the greatest amount of production of VFAs and LA, and three groups of $S/I = 1:2$ (T2), $S/I = 1:3$ (T3), and $S/I = 1:4$ (T4) with relatively high yield of methane.

3.2.1. Composition and variation of the bacterial community

To investigate the diversity of bacterial communities in the AD process between each group, a statistical evaluation was performed using the Sobs and Shannon indices. The Sobs index is adopted to assess the abundance of communities, while the Shannon index is usually applied to characterize the diversity of communities. The Sobs index of T1 was 577.17, which was significantly lower than those of T2, T3, and T4 (674.50, 685.75, and 679.00 respectively) (Fig. 3a) ($P < 0.05$). Typically, a more severe environment leads to simpler communities (Vasconcelos et al., 2016). The pH of T1 was approximately 4.55–4.70 in the early stage, even if there were more substrates, it was not conducive to the metabolic growth of most anaerobic microorganisms (Ma et al.,

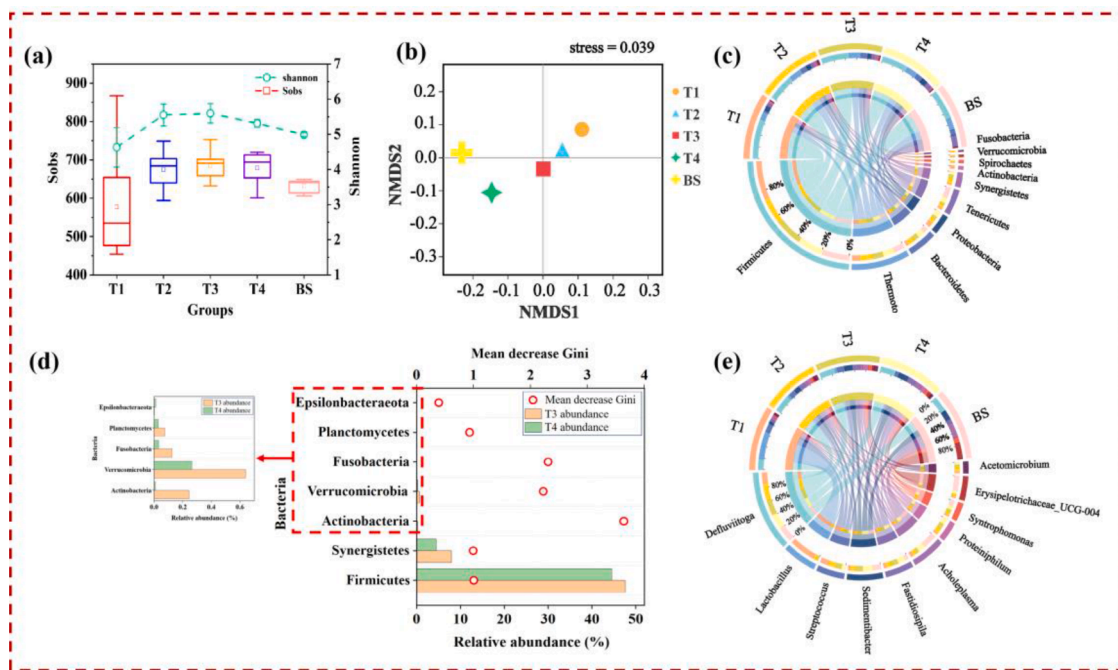


Fig. 3. The bacterial communities analysis. (a) Alpha diversity. (b) Unweighted UniFrac metrics NMDS (non-metric multidimensional scaling) analysis. (c) The abundance of bacteria at the phylum level. (d) Feature importance and relative abundance of bacteria in T3 and T4 at the phylum level. (e) The abundance of bacteria at the genus level.

2019b). The Sobs index increased with the increase in inoculum. Interestingly, this index reached its maximum at $S/I = 1:3$ and then decreased again at $S/I = 1:4$, which indicated that the $S/I = 1:3$ condition was the most suitable for the growth and reproduction of most bacteria. The Shannon index of T3 was also the highest among all of the groups (5.60), which demonstrated that the substrate in T3 can be rapidly degraded by more varied hydrolytic and acidogenic bacteria in comparison with T4 to provide more abundant available substrate for the metabolism of methanogens. Zheng et al. (2021) also demonstrated that the bacterial communities with higher diversity and uniformity contribute to the more efficient methane production. A non-metric multidimensional scale (NMDS) analysis can typically reflect the differences of communities between groups, and its accuracy is usually evaluated by its stress value. Typically, a stress value < 0.1 indicates that the model is more reliable, and it was 0.039 in this study. The community distribution differed significantly between groups ($P < 0.05$), which demonstrated that the S/I ratio could significantly affect the distribution between bacterial communities. The influence of the S/I ratio on the structure of bacterial community was caused by the interaction between microorganisms, intermediate substrates, and environmental factors.

The dominant bacteria at the phylum level primarily included *Firmicutes*, *Thermotogae*, *Bacteroidetes*, *Proteobacteria*, *Tenericutes*, *Synergistetes*, *Actinobacteria*, and others (Fig. 3c). All of these are known to dominate the processes of hydrolysis and acidogenesis in AD (Dykstra and Pavlostathis., 2017; Wang et al., 2018). The abundance of *Firmicutes* in T1 was the highest (65.11%) among all the groups ($P < 0.05$). Amin et al. (2021) revealed that *Firmicutes* can produce spores to resist extreme environments and then become the dominant bacteria in the community. In contrast, the acidic environment caused a decrease in the community diversity of T1, whereas *Firmicutes* adapted to it and became the predominant microbe. As the proportion of inoculum increased (T3 and T4), the abundances of hydrolytic and acidogenic dominant bacteria increased significantly, primarily *Thermotogae*, *Bacteroidetes*, and *Synergistetes*, which can hydrolyze and transform organic matter (Yang et al., 2021). Interestingly, the abundances of *Bacteroidetes* and *Synergistetes* reached their maximum at $S/I = 1:3$, which were 11.31% and

7.95%, respectively. Relevant studies have shown that *Bacteroidetes* and *Synergistetes* can degrade glucose, cellobiose, and amino acids to VFAs, CO_2 , and H_2 , respectively (Dykstra and Pavlostathis., 2017; Si et al., 2016). Moreover, the enrichment of *Bacteroidetes* and *Synergistetes* could provide potent support to the methane metabolism of methanogens in T3 (Lee et al., 2020; Yang et al., 2021).

T3 and T4 were both relatively high methanogenic groups. To further investigate the difference in bacterial composition between the two groups and identify the critical microorganisms, a random forest was utilized to perform an algorithm analysis on the community composition at the phylum level (Fig. 3d). Moreover, mean decrease gini (MDG) was introduced to evaluate the importance of the bacteria. Typically, a larger Gini indicates that the bacteria are more important to the system (Long et al., 2021). The MDG of the phyla *Actinobacteria*, *Fusobacteria*, *Verrucomicrobia*, *Firmicutes*, and *Synergistetes* were the top 5 in system, which indicated that these bacteria played significant roles in the process of AD. Importantly, in contrast to T4, all of these microorganisms were more abundant in T3. Interestingly, although the abundance of *Actinobacteria* was only 0.24%, its MDG was the highest among all the bacteria, which showed that the less abundant microbe was also critical in determining the performance of AD. Nguyen et al. (2019) reported that *Actinobacteria* was responsible for the conversion of polysaccharides and proteins to acetic acid, propionic acid, and H_2 , which provided the substrates for methanogenesis. The MDG of *Fusobacteria* and *Verrucomicrobia* were 2.31 and 2.23, respectively; these bacteria were involved in hydrolysis and acidogenesis and could degrade organic compounds to VFAs (Ma et al., 2019a; Qiu et al., 2014). Additionally, *Firmicutes* and *Synergistetes* have been proven to provide powerful support for the stable operation of AD (Wang et al., 2018). Patil et al. (2021) suggested that the bacteria assigned to these phyla helped to establish a syntrophic relationship with methanogens and targeted the conversion of various organic compounds, such as glucose, lignocellulose, and proteins to acetic acid and H_2 .

Fig. 3e shows the bacterial community composition at the genus level. *Lactobacillus* was the most abundant bacteria in T1 (33.94%), which was significantly higher than those of the other three groups ($P < 0.05$). *Lactobacillus* could target the conversion of carbohydrates that are

rich in T1 to LA (Wang et al., 2020). The T2, T3, and T4 community contained a large amount of *Deftuviitoga*, which can degrade cellulose into acetic acid, H₂, and CO₂ (Hania et al., 2012). The hydrolysis of cellulose plays an important role in the rate-limiting step of the hydrolysis of organic matter. Therefore, the K_d of the low S/I ratios was the highest. The abundances of *Proteiniphilum* and *Acetomicrobium* were the highest in T3 and were affiliated with the *Bacteroidetes* and *Synergistetes* phyla. These two genera can convert complex organic matter, thus, continuously providing substrates for the subsequent production of methane (Wang et al., 2021a).

3.2.2. Composition and variation of the archaeal community

Compared with the bacterial community, the community diversity and richness of the archaea were much lower (Fig. 4a). The Sobs and Shannon indices of T3 and T4 were the highest, and there was no significant difference between them ($P > 0.05$). However, the methane production of T3 was significantly higher than that of T4, which was primarily owing to the sufficient levels of available substrate and the higher abundance of *Synergistetes* in T3 (Fig. 3a). Since *Synergistetes* has been proven to be an electrochemically active bacterium that can participate in interspecies electron transfer (IET) and establish syntrophic metabolism with hydrogenotrophic methanogens, such as *Methanobacterium* and *Methanospirillum*, it thereby contributes to the stimulation of methane production (Yang et al., 2021). The NMDS analysis of the stress of archaea was 0.030 in this study (Fig. 4b). No significant difference was observed in the distribution of archaeal communities between T1 and T2 ($P = 0.332$), which may be due to the selection pressure from high concentrations VFA. The similar microbial concentration and buffer system in T3 and T4 may account for the lack of difference in the distribution of archaeal communities between them

($P = 0.961$) (Meng et al., 2018). Therefore, differences between the two methanogenic processes need to be further characterized from the metabolic pathways.

Euryarchaeota was the dominant archaea at the phylum level of each group (Fig. 5c). Most methanogens that are members of *Euryarchaeota*. *Methanobacterium*, *Methanosarcina*, *Methanoculleus*, and *Methanospirillum* were the dominant archaea at the genus level (Fig. 4d), and their relative abundance among each group > 90%. Among them, *Methanobacterium*, *Methanoculleus*, and *Methanospirillum* are hydrogenotrophic methanogens and can only use H₂ and CO₂ for methanogenesis. *Methanosarcina* can simultaneously utilize H₂ and acetate for methane metabolism (Dykstra and Pavlostathis., 2017). The abundance of *Methanobacterium* in T3 and T4 was 75.11% and 60.53%, respectively, which indicated that hydrogenotrophic methanogenesis was the primary methanogenesis pathway. *Methanosarcina* in T4 was the most abundant (20.86%), which was higher than that in T3. Wang et al., 2021b found that *Methanosarcina* is better suited for survival in a high acetic acid environment. Before day 2, the acetic acid content of T4 was significantly higher than that of other groups (Fig. 2i). In particular, *Methanospirillum* was the most abundant in T3 and was the highest at 8.45%. Jing et al. (2017) revealed that *Methanospirillum* can be involved in the direct interspecies electron transfer (DIET) by the reduction of CO₂ in methane metabolism, thus, effectively enhancing the performance of AD. This signified that the enrichment with *Methanospirillum* in T3 enhanced the stimulation of methane production.

3.2.3. Analysis of microbial correlation network under different S/I ratios

When the $P < 0.05$ between two microbes, the relationship between microorganisms is presented in the network (Fig. 5). *Lactobacillus* was negatively correlated with most of the genera in this network, which

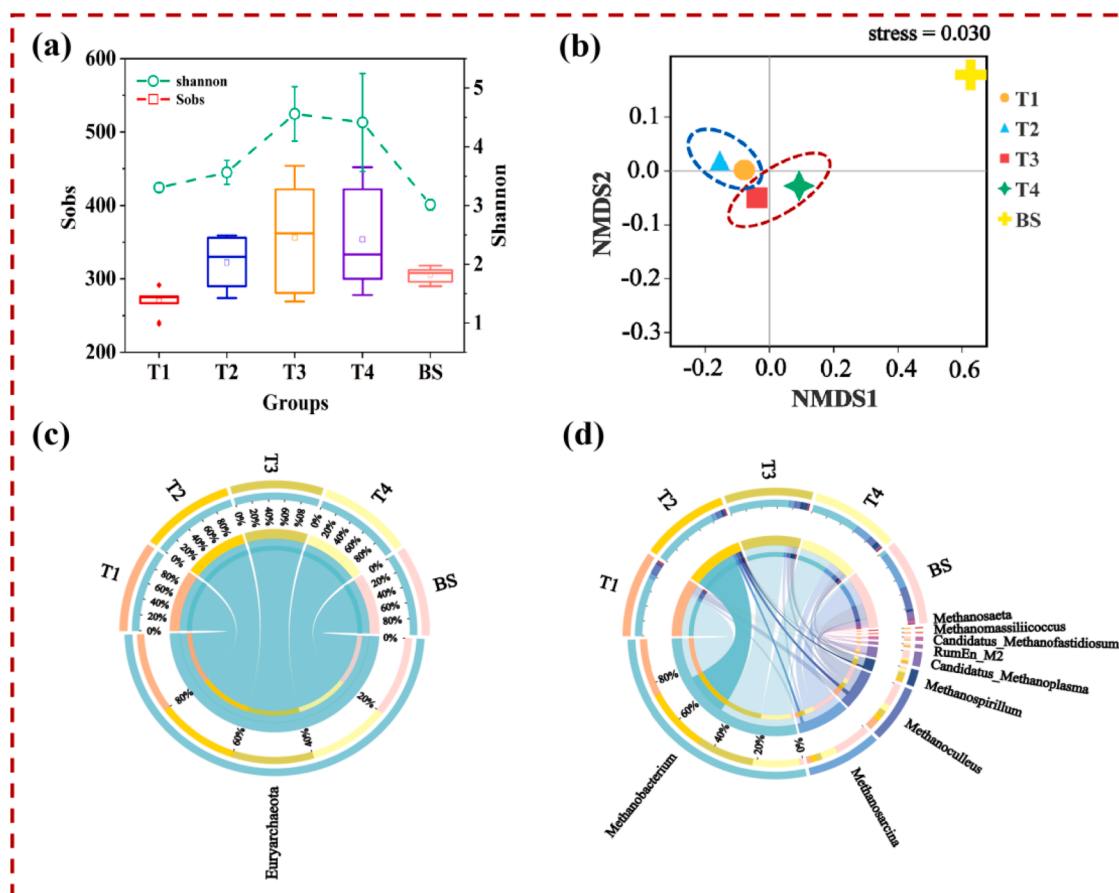


Fig. 4. The archaeal community analysis (a) Alpha diversity. (b) Unweighted UniFrac metrics NMDS analysis. The abundance of archaea at the (c) phylum and (d) genus level.

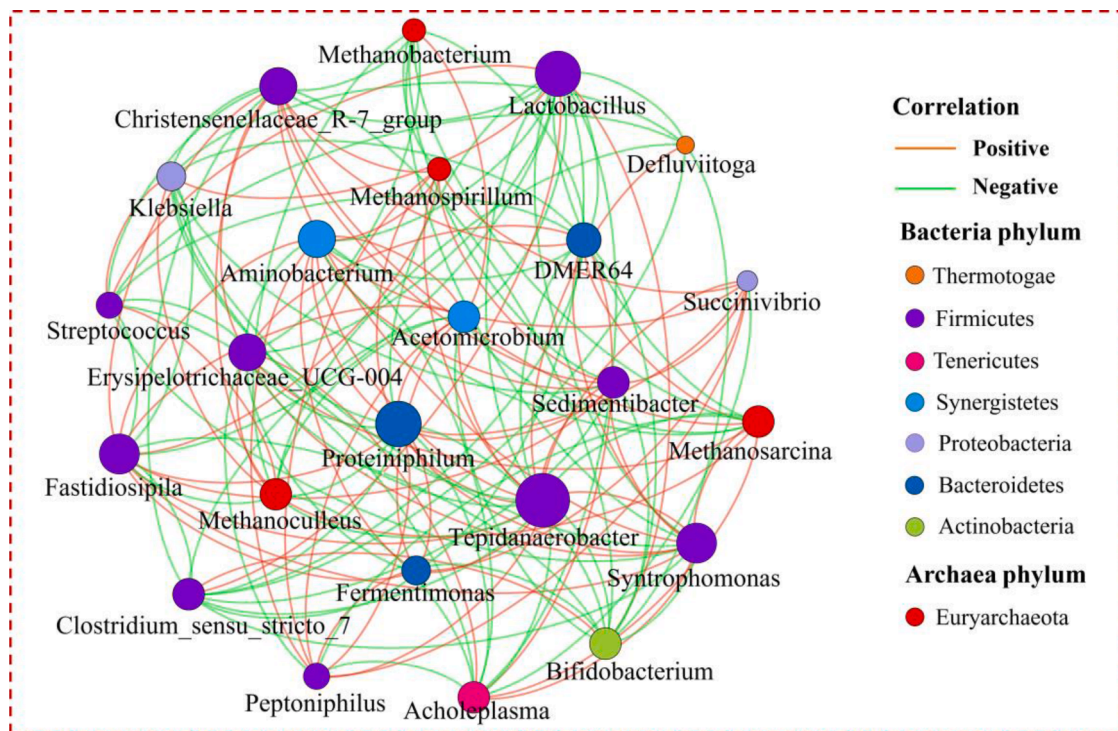


Fig. 5. The analysis of microbial correlation network at the genus level (Note: When the correlation coefficient > 0 , the color of the connecting line is orange, indicating that there is a positive correlation between the two microorganisms. When the correlation < 0 , the line is green, demonstrating a negative correlation among the two microbes.).

showed that there was a competitive relationship between *Lactobacillus* and the most connected microbes. *Proteiniphilum* significantly positively correlated with *Fastidiosipila*, *Tepidanaerobacter*, *Aminobacterium*, and *Acetomicrobium*, which were all abundant in T3 (Table. S1). This implied that they exhibited a cooperative relationship among them, which can synergistically promote the decomposition of small molecular organic substances, thereby providing sufficient nutrient substrates for the metabolism of methanogens in T3 (Wang et al., 2020; Wang et al., 2021a).

As for the analysis of the correlation between bacteria and archaea, *Syntrophomonas* was positively related with *Methanosarcina*. *Syntrophomonas* has been confirmed to be a type of syntrophic acetate-oxidizing bacteria (SAOB) that can quickly convert H_2 and CO_2 into acetic acid and then further catalyze it to methane by acetoclastic methanogens, such as *Methanosarcina* (Kurade et al., 2019). *Tepidanaerobacter* is classified under the Firmicutes, which was related to 20 types of microorganisms in the network. Tsavkelova et al. (2018) revealed that *Tepidanaerobacter* was a SAOB, which was closely related to most hydrothermophilic methanogens. *Tepidanaerobacter* and *Methanospirillum* positively correlated in this network, and their abundances were the highest in T3 (1.65% and 8.45%, respectively). This implied that *Tepidanaerobacter* could convert acetic acid into H_2 and CO_2 and facilitate the syntrophic acetate oxidation-hydrogenotrophic methanogenesis pathway, which aids in the production of methane in T3. *Acetomicrobium* was the only genus that was positively related to *Methanobacterium* in this network, indicating that the presence of *Acetomicrobium* could support the growth of *Methanobacterium*.

Overall, in the high S/I ratio (T1), the stress-resistant groups that primarily contain *Lactobacillus* were significantly enriched to adapt to severe environments, and the negative correlation between microorganisms was more apparent, which was the vital driving factor to inhibit the production of methane. In contrast, the microorganisms in the low S/I ratios, particularly in T3, had more synergistic relationships with each other. In particular, these microorganisms were likely to implement a unique niche in the system and affect the shift of overall

metabolic pathway to the syntrophic metabolism pathway, which contributed to methanogenesis.

3.3. Analysis of the entire metabolic pathway in AD

3.3.1. Prediction of metabolic functions under different S/I ratios in the AD process

The metabolic function of AD microbial communities under different S/I ratios was predicted using Tax4Fun (Fig. 6). Metabolism, genetic information processing, environmental information processing, and cellular process was the four main metabolic pathways in each group (Fig. 6a). The primary secondary metabolic pathways in T3, which were 7.23%, 7.69%, and 6.04%, respectively, were amino acid metabolism, energy metabolism, and metabolism of cofactors and vitamins. These values were significantly higher than those of the other groups ($P < 0.05$) (Fig. 6a-6b). These metabolic pathways were closely related to *Proteiniphilum*, *Acetomicrobium*, and *Methanobacterium* (Wang et al., 2020). This showed that the amino acid metabolism led by *Proteiniphilum* provides a rich nutrient substrate for methanogens, while cofactors and vitamins can promote the catalytic reaction of cell functional enzymes, thereby accelerating the anaerobic reaction process (Fan et al., 2020). In addition, the cell motility in T3 was significantly higher than those of the other groups ($P < 0.05$). Jarrell and Albers (2012) demonstrated that the high levels of motility in methanogens are due to possession of multiple flagellae. Town and Dumonceaux (2016) demonstrated that some genes that encode methanogenesis were also closely related to cell motility. This indicated that the metabolic activity of methanogens in T3 was relatively higher. The abundances of translation (17.31%) and cell growth and death (2.63%) in T2 were the highest, which was consistent with the previous maximum K_d of S/I = 1:2. Further analysis illustrated that the metabolism of methane in T3 was significantly higher than those of the other groups ($P < 0.05$) (Fig. 6c), indicating that the activity of methanogenic archaea in T3 might be higher than those of other groups.

Overall, the results demonstrated that the pathway of carbohydrate

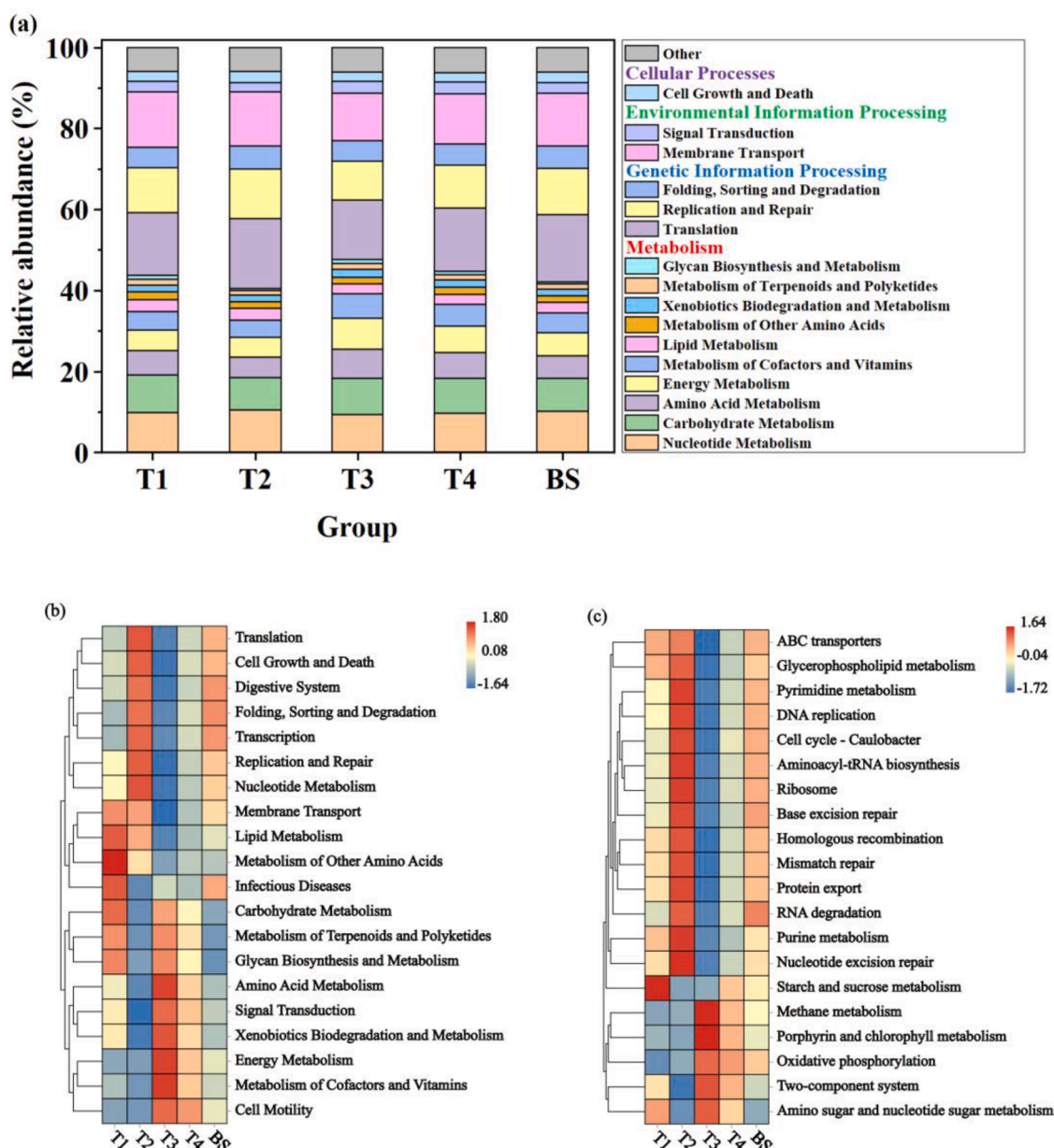


Fig. 6. Microbial metabolism function profiles of each group in AD (relative abundance > 1.0%): (a) Function categories. (b) Level 2 metabolic function heat map analysis. (c) Level 3 metabolic function heat map analysis.

and amino acid metabolism in T3 dominated the hydrolysis process, providing sufficient available substrates for subsequent acidogenesis, moreover, the variation in pH was stable (Fig. 2h). Vigorous energy metabolism provided a potent guarantee for the consumption of energy in T3. In addition, active cofactors effectively promoted the transfer of electrons and groups in the enzymatic reactions, thereby accelerating the AD process. Thus, the coordination of different levels of metabolism convincingly facilitate the production of methane in T3.

3.3.2. Analysis of the key metabolic pathways under different S/I ratios

To clearly reflect the key metabolic pathways of the optimal S/I ratio, the functional metabolic analyses from hydrolysis, acidogenesis, and methanogenesis of each group was identified using the combination of Tax4Fun and KEGG metabolic pathways (Fig. 7).

The abundances of alpha-glucosidase were the highest in T1 (Fig. 7a), which indicated that the conversion of starch to pyruvate were the major hydrolysis pathways. The abundances of endoglucanase and

protease were higher in T3 and T4 (Fig. 7a), which demonstrated that bacteria that can degrade protein and cellulose were more abundant. Zou et al., 2020 clarified that the enrichment of *Bacteroidetes* was specifically favorable to degrade protein and cellulose. In particular, *Bacteroidetes* was more abundant in T3 and T4 (Fig. 3).

During acidogenesis, pyruvate produced by glycolysis is reduced to LA by lactate dehydrogenase, and the LA is then degraded to propionate by propionate CoA-transferase during AD (Zhou et al., 2018). Levels of L-lactate/D-lactate dehydrogenase and propionate CoA-transferase were higher in T1 than in the other groups. As shown in Fig. 2, LA was the initial product of anaerobic digestion at high S/I ratios, which was faster than the generation of VFAs, and reached a peak by day 2. The relative abundance of L-lactate/D-lactate dehydrogenase suggests that the LA produced in each group may have been mainly L-lactic acid. T1 contained higher levels of glucose than the other groups and was rich in *Lactobacillus*, leading to the observed high LA levels. Over time, some of the LA may be converted to propionic acid by propionate

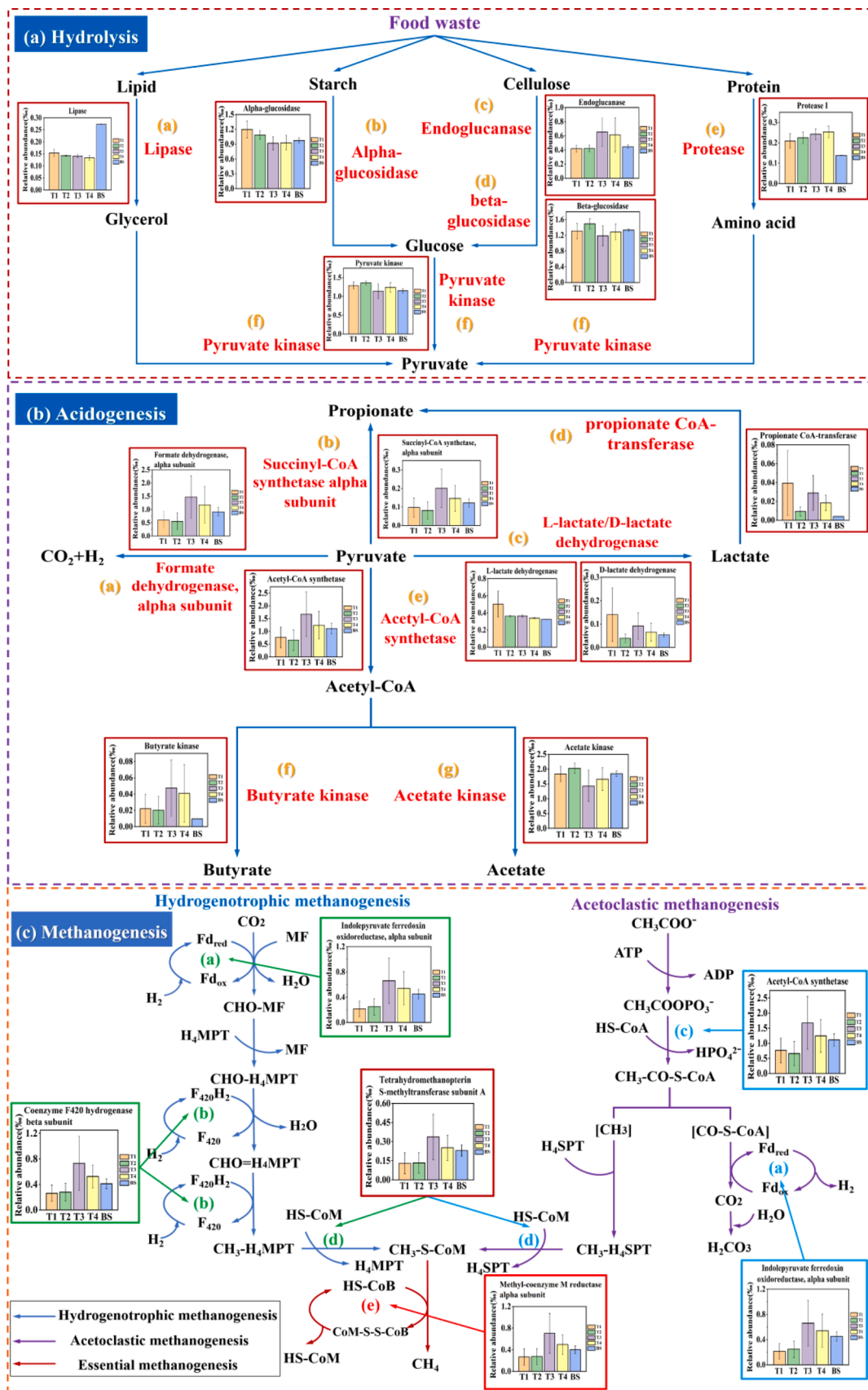


Fig. 7. The variations in the abundances of key enzymes-encoding genes related to (a) hydrolysis, (b) acidogenesis, and (c) methanogenesis at each group.

CoA-transferase. In addition, the contents of propionic acid of T1 and T2 were significantly higher than those of T3 and T4 ($P < 0.05$) (Fig. 2). On the one hand, the excessive accumulation of propionic acid can significantly inhibit the metabolic activity of methanogens. Alternatively, the Gibbs free energy required for the conversion of propionic acid to acetic acid and H_2 was higher ($T = 35^\circ\text{C}$, $\text{pH}=7$, 1 atm. $\text{CH}_3\text{CH}_2\text{COO}^- + 3\text{H}_2\text{O} \rightarrow \text{CH}_3\text{COO}^- + \text{HCO}_3^- + 3\text{H}_2 + \text{H}^+ \Delta G^0 = +76.1 \text{ KJ/mol}$) (Li et al., 2020), which was the slowest in the conversion of all of the VFAs to acetic acid and H_2 . Therefore, the methane production of T1 and T2 were lower than those of T3 and T4. Importantly, pyruvate kinase and acetate kinase were responsible for the metabolic pathways of acetate production, and it was observed that their levels in T1 and T2 were higher than those in T3 and T4. Although the acetic acid contents of T3 and T4 in the early stage were higher than those of T1 and T2, a large amount of acetic acid was consumed by *Methanosarcina* to generate CH_4 , while some accumulation occurred in T1 and T2.

The key enzyme-encoding genes related to methanogenesis in T3 and T4 were obviously higher than those in T1 and T2 (Fig. 7c), indicating that appropriately reducing the S/I ratio can significantly facilitate the metabolic function of methanogens. The abundance of formate dehydrogenase, alpha subunit was significantly higher in T3 during acidogenesis than in the other groups ($P < 0.05$) (Fig. 7b). Formate C-acetyltransferase catalyzes the breakdown of pyruvate to formic acid, whereas formate dehydrogenase promotes the decomposition of formic acid into H_2 and CO_2 (Guo et al., 2015; Wang et al., 2021b). These reactions support the methane metabolism by hydrogenotrophic methanogens in T3. Other key enzymes in the hydrogenotrophic methanogenic pathway include indolepyruvate ferredoxin oxidoreductase alpha subunit and coenzyme F420 hydrogenase, beta subunit, which target the reduction of CO_2 to formyl, methylene, and methyl groups using H_2 as electron donors. Methyl groups are further converted to $\text{CH}_3\text{-S-CoM}$ (methyl-CoM) under the action of tetrahydromethylopterin S-methyltransferase subunit A, and finally reduced to CH_4 by the methyl coenzyme M reductase alpha subunit (Fang et al., 2015; Guo et al., 2015). In the acetoclastic pathway, acetic acid is first converted to acetyl-coenzyme A by a variety of enzymes such as acetyl-CoA synthetase. Acetyl-CoA synthetase was most abundant in T3, thus promoting the synthesis of acetyl-CoA. Zheng et al. (2021) observed that higher levels of acetyl-CoA synthetase are associated with more acetoclastic methanogenesis. Subsequently, acetyl-coenzyme A is catalyzed by the carbon monoxide dehydrogenase/acetyl-CoA synthase complex to generate methyl with Fd_{ox} (ferredoxin) as an electron acceptor, which is then converted to CH_4 through tetrahydromethanopterin S-methyltransferase and methyl-coenzyme M reductase (Fang et al., 2015; Guo et al., 2015). Tetrahydromethanopterin S-methyltransferase subunit A and methyl-coenzyme M reductase alpha subunit are the key enzymes shared by all the metabolic pathways of methanogenesis. It is worth noting that the abundances of key enzyme-encoding genes in both the hydrogenotrophic and acetoclastic methanogenesis pathways were the highest in T3. This also directly confirmed that S/I = 1:3 was the most conducive to the production of methane.

4. Conclusions

This study systematically investigated the influence of S/I ratios on the overall AD process and elucidated the microbial interactions and entire metabolic pathways under the optimal S/I ratio. The results suggest that the acid suppression phenomenon was problematic in high S/I ratios, while the low S/I ratios were associated with the production of methane. An additional kinetic analysis illustrated that S/I = 1:3 had the largest methane yield. As the S/I gradually decreased, the abundance and diversity of bacteria and archaea increased. In particular, they were exceptionally high in S/I = 1:3. The enrichment of *Synergistetes* and *Bacteroidetes* in S/I = 1:3, which helped to establish a syntrophic relationship with hydrogenotrophic methanogens. Furthermore, microbial cooperation was higher at S/I = 1:3. The abundances of all the key

enzyme-encoding genes in the methanogenesis pathway under S/I = 1:3 were the highest. Taken together, this information will assist the determination of the synergistic and antagonistic mechanisms of substrate and inoculum in AD to guide the rapid start-up and directional control of the batch AD of FW.

Declaration of Competing Interest

The authors declare that they have no known competing financial interests or personal relationships that could have appeared to influence the work reported in this paper.

Acknowledgements

This research was supported by the National Key R&D Program of China (Grant number: 2018YFC1901000), the Natural Science Foundation of China (Grant number: 52070177), the Key Natural Science Foundation of Fujian (Grant number: 2020J02009), and the Ningbo Public Welfare Science and Technology Plan Project (Grant number: 2021S115). The authors also thank mjeditor (www.mjeditor.com) for its linguistic assistance during the preparation of this manuscript.

Supplementary materials

Supplementary material associated with this article can be found, in the online version, at doi:10.1016/j.watres.2022.118440.

References

- Amin, F.R., Khalid, H., El-Mashad, H.M., Chen, C., Liu, G., Zhang, R., 2021. Functions of bacteria and archaea participating in the bioconversion of organic waste for methane production. *Sci. Total Environ.* 763, 143007.
- APHA, 2005. Standard Methods for the Examination of Water and Wastewater. American Public Health Association, Washington, DC, USA.
- Chen, Z., Li, Y., Peng, Y., Ye, C., Zhang, S., 2021. Effects of antibiotics on hydrolase activity and structure of microbial community during aerobic co-composting of food waste with sewage sludge. *Bioresour. Technol.* 321, 124506.
- Cho, H.S., Moon, H.S., Lim, J.Y., Kim, J.Y., 2013. Effect of long chain fatty acids removal as a pretreatment on the anaerobic digestion of food waste. *J. Mater. Cycles Waste Manag.* 15, 82–89.
- Dykstra, C.M., Pavlostathis, S.G., 2017. Methanogenic biocathode microbial community development and the role of bacteria. *Environ. Sci. Technol.* 51 (9), 5306–5316.
- Fang, X., Li, J., Rui, J., Li, X., 2015. Research progress in biochemical pathways of methanogenesis. *Chin. J. Appl. Environ. Biol.* 21 (1), 1–9.
- Fan, Y., Niu, X., Zhang, D., Lin, Z., Fu, M., Zhou, S., 2020. Analysis of the characteristics of phosphine production by anaerobic digestion based on microbial community dynamics, metabolic pathways, and isolation of the phosphate-reducing strain. *Chemosphere* 262, 128213.
- Guo, J.H., Peng, Y.Z., Ni, B.J., Han, X.Y., Fan, L., Yuan, Z.G., 2015. Dissecting microbial community structure and methane-producing pathways of a full-scale anaerobic reactor digesting activated sludge from wastewater treatment by metagenomic sequencing. *Microb. Cell Fact.* 14, 33.
- Hania, W.B., Godbane, R., Postec, A., Hamdi, M., Ollivier, B., Fardeau, M.L., 2012. *Defluviitoga tunisiensis* gen. nov., sp. nov., a thermophilic bacterium isolated from a mesothermic and anaerobic whey digester. *Int. J. Syst. Evol. Microbiol.* 62 (6), 1377–1382.
- Holliger, C., Alves, M., Andrade, D., Angelidaki, I., Astals, S., Baier, U., et al., 2016. Towards a standardization of biomethane potential tests. *Water Sci. Technol.* 74, 2515–2522.
- Jarrell, K.F., Albers, S.V., 2012. The archaeum: an old motility structure with a new name. *Trends Microbiol.* 20 (7), 307–312.
- Jing, Y., Wan, J., Angelidaki, I., Zhang, S., Luo, G., 2017. iTRAQ quantitative proteomic analysis reveals the pathways for methanation of propionate facilitated by magnetite. *Water Res* 108, 212–221.
- Khadka, A., Parajuli, A., Dangol, S., Thapa, B., Sapkota, L., Carmona-Martínez, A.A., Ghimire, A., 2022. Effect of the Substrate to Inoculum Ratios on the Kinetics of Biogas Production during the Mesophilic Anaerobic Digestion of Food Waste. *Energies* 15, 834.
- Kong, X., Xu, S., Liu, J., Li, H., Zhao, K., He, L., 2016. Enhancing anaerobic digestion of high-pressure extruded food waste by inoculum optimization. *J. Environ. Manage.* 166, 31–37.
- Kurade, M.B., Saha, S., Salama, E.-S., Patil, S.M., Govindwar, S.P., Jeon, B.-H., 2019. Acetoclastic methanogenesis led by *Methanosarcina* in anaerobic co-digestion of fats, oil and grease for enhanced production of methane. *Bioresour. Technol.* 272, 351–359.
- Lee, H.S., Salerno, M.B., Rittmann, B.E., 2008. Thermodynamic evaluation on H_2 production in glucose fermentation. *Environ. Sci. Technol.* 42 (7), 2401–2407.

- Lee, J., Hong, J., Jeong, S., Chandran, K., Park, K.Y., 2020. Interactions between substrate characteristics and microbial communities on biogas production yield and rate. *Bioresour. Technol.* 303, 122934.
- Li, L., He, Q., Zhao, X., Wu, D., Wang, X., Peng, X., 2018a. Anaerobic digestion of food waste: correlation of kinetic parameters with operational conditions and process performance. *Biochem. Eng. J.* 130, 1–9.
- Li, Q., Liu, Y., Yang, X., Zhang, J., Lu, B., Chen, R., 2020. Kinetic and thermodynamic effects of temperature on methanogenic degradation of acetate, propionate, butyrate and valerate. *Chem. Eng. J.* 396, 125366.
- Li, Y., Jin, Y., Borrin, A., Li, J., 2018b. Influence of feed/inoculum ratios and waste cooking oil content on the mesophilic anaerobic digestion of food waste. *Waste Manag* 73, 156–164.
- Lin, L., Xu, F., Ge, X., Li, Y., 2018. Improving the sustainability of organic waste management practices in the food-energy-water nexus: a comparative review of anaerobic digestion and composting. *Renew. Sustain. Energy Rev.* 89, 151–167.
- Long, F., Wang, L., Cai, W., Lesnik, K., Liu, H., 2021. Predicting the performance of anaerobic digestion using machine learning algorithms and genomic data. *Water Res* 199, 117182.
- Lu, J., Xu, S., 2021. Post-treatment of food waste digestate towards land application: a review. *J. Clean. Prod.* 303, 127033.
- Ma, K., Cao, Z., Cui, Y., Chen, T., Lv, J., 2021. Effect of magnetite on anaerobic digestion treating saline wastewater: methane production, biomass aggregation and microbial community dynamics. *Bioresour. Technol.* 341 (17), 125783.
- Ma, S.-J., Ma, H.-J., Hu, H.-D., Ren, H.-Q., 2019a. Effect of mixing intensity on hydrolysis and acidification of sewage sludge in two-stage anaerobic digestion: characteristics of dissolved organic matter and the key microorganisms. *Water Res* 148, 359–367.
- Ma, X., Jiang, T., Chang, J., Tang, Q., Cui, Z., 2019b. Effect of substrate to inoculum ratio on biogas production and microbial community during semi-solid-state batch anaerobic co-digestion of rape straw and dairy manure. *Appl. Biochem. Biotechnol.* 189, 884–902.
- Mao, C., Wang, X., Xi, J., Feng, Y., Ren, G., 2017. Linkage of kinetic parameters with process parameters and operational conditions during anaerobic digestion. *Energy* 135, 352–360.
- Meng, L., Xie, L., Kinh, C.T., Suenaga, T., Hori, T., Riya, S., Terada, A., Hosomi, M., 2018. Influence of feedstock-to-inoculum ratio on performance and microbial community succession during solid-state thermophilic anaerobic co-digestion of pig urine and rice straw. *Bioresour. Technol.* 252, 127–133.
- Nguyen, L.N., Mohammed, J.A.H., Commault, A., Bustamante, H., Nghiem, L.D., 2019. Impacts of mixing on foaming, methane production, stratification and microbial community in full-scale anaerobic co-digestion process. *Bioresour. Technol.* 281, 226–223.
- Patil, S.M., Kurade, M.B., Basak, B., Saha, S., Jeon, B.H., 2021. Anaerobic co-digester microbiome during food waste valorization reveals *Methanosaeta* mediated methanogenesis with improved carbohydrate and lipid metabolism. *Bioresour. Technol.* 332, 125123.
- Qiu, Y.-L., Kuang, X.-Z., Shi, X.-S., Yuan, X.-Z., Guo, R.-B., 2014. *Terrimicrobium sacchariphilum* gen. nov., sp. nov., an anaerobic bacterium of the class 'spartobacteria' in the phylum *Verrucomicrobia*, isolated from a rice paddy field. *Int. J. Syst. Evol. Microbiol.* 64 (5), 1718–1723.
- Si, B., Liu, Z., Zhang, Y., Li, J., Shen, R., Zhu, Z., Xing, X., 2016. Towards biohythane production from biomass: influence of operational stage on anaerobic fermentation and microbial community. *Int. J. Hydrog. Energy* 41 (7), 4429–4438.
- Tang, J., Wang, X.C., Hu, Y., Zhang, Y., Li, Y., 2017. Effect of pH on lactic acid production from acidogenic fermentation of food waste with different types of inocula. *Bioresour. Technol.* 224, 544–552.
- Town, J.R., Dumonceaux, T.J., 2016. Laboratory-scale bioaugmentation relieves acetate accumulation and stimulates methane production in stalled anaerobic digesters. *Appl. Microbiol. Biotechnol.* 100, 1009–1017.
- Tsavelkova, E., Prokudina, L., Egorova, M., Leontieva, M., Malakhova, D., Netrusov, A., 2018. The structure of the anaerobic thermophilic microbial community for the bioconversion of the cellulose-containing substrates into biogas. *Process. Biochem.* 66, 183–196.
- Vasconcelos, E.A.F., Leitão, R.C., Santaella, S.T., 2016. Factors that affect bacterial ecology in hydrogen-producing anaerobic reactors. *Bioenergy Res* 9 (4), 1260–1271.
- Wang, B., Ma, J., Zhang, L., Su, Y., Xie, Y., Ahmad, Z., et al., 2021a. The synergistic strategy and microbial ecology of the anaerobic co-digestion of food waste under the regulation of domestic garbage classification in China. *Sci. Total Environ.* 765, 144632.
- Wang, P., Qiao, Z., Li, X., Su, Y., Xie, B., 2020. Functional characteristic of microbial communities in large-scale biotreatment systems of food waste. *Sci. Total Environ.* 746, 141086.
- Wang, P., Wang, H., Qiu, Y., Ren, L., Jiang, B., 2018. Microbial characteristics in anaerobic digestion process of food waste for methane production-A review. *Bioresour. Technol.* 248, 29–36.
- Wang, R., Li, C., Lv, N., Pan, X., Cai, G., Ning, J., Zhu, G., 2021b. Deeper insights into effect of activated carbon and nano-zero-valent iron addition on acidogenesis and whole anaerobic digestion. *Bioresour. Technol.* 324, 124671.
- Wu, Q.-L., Guo, W.-Q., Zheng, H.-S., Luo, H.-C., Feng, X.-C., Yin, R.-L., Ren, N.-Q., 2016. Enhancement of volatile fatty acid production by co-fermentation of food waste and excess sludge without pH control: the mechanism and microbial community analyses. *Bioresour. Technol.* 216, 653–660.
- Xing, B., Cao, S., Han, Y., Wen, J., Zhang, K., Wang, X.C., 2020. Stable and high-rate anaerobic co-digestion of food waste and cow manure: optimisation of start-up conditions. *Bioresour. Technol.* 307, 123195.
- Yang, S., Chen, Z., Wen, Q., 2021. Impacts of biochar on anaerobic digestion of swine manure: methanogenesis and antibiotic resistance genes dissemination. *Bioresour. Technol.* 324, 124679.
- Zhang, W., Lang, Q., Fang, M., Li, X., Bah, H., Dong, H., Dong, R., 2017. Combined effect of crude fat content and initial substrate concentration on batch anaerobic digestion characteristics of food waste. *Bioresour. Technol.* 232, 304–312.
- Zheng, Z., Cai, Y., Zhang, Y., Zhao, Y., Gao, Y., Cui, Z., Hu, Y., Wang, X., 2021. The effects of C/N (10-25) on the relationship of substrates, metabolites, and microorganisms in "inhibited steady-state" of anaerobic digestion. *Water Res* 188, 116466.
- Zhou, M., Yan, B., Wong, J., Zhang, Y., 2018. Enhanced volatile fatty acids production from anaerobic fermentation of food waste: a mini-review focusing on acidogenic metabolic pathways. *Bioresour. Technol.* 248, 68–78.
- Zhou, J., Zhang, R., Liu, F., Yong, X., Wu, X., Zheng, T., Jiang, M., Jia, H., 2016. Biogas production and microbial community shift through neutral pH control during the anaerobic digestion of pig manure. *Bioresour. Technol.* 217, 44–49.
- Zou, H., Jiang, Q., Zhu, R., Chen, Y., Sun, T., Li, M., Zhai, J., Shi, D., Ai, H., Gu, L., He, Q., 2020. Enhanced hydrolysis of lignocellulose in corn cob by using food waste pretreatment to improve anaerobic digestion performance. *J. Environ. Manag.* 254, 109830.